W-12,792

ORNL-TM-3628

NTIS HC $3.75

Dupe of

BIOLOGY DIVISION
HABROBRACON EXPERIMENT P-1079
ANNUAL PROGRESS REPORT

to the

National Aeronautics and Space Administration

January 1 - December 31, 1968

(NASA-CR-127142) BIOLOGY DIVISION HABROBRACON EXPERIMENT P-1079 Annual Report, 1 Jan. - 31 Dec. 1968 (Oak Ridge National Lab.) 31 Dec. 1968 35 p CSCL 06R G3/04

N73-13082

Unclas 49544

OAK RIDGE NATIONAL LABORATORY

OPERATED BY UNION CARBIDE CORPORATION • FOR THE U.S. ATOMIC ENERGY COMMISSION

ORNL-TM- 3628

BIOLOGY DIVISION
HABROBRACON EXPERIMENT P-1079
ANNUAL PROGRESS REPORT
TO THE
NATIONAL AERONAUTICS AND SPACE ADMINISTRATION

January 1 - December 31, 1968

OAK RIDGE NATIONAL LABORATORY
Oak Ridge, Tennessee 37830
operated by
UNION CARBIDE CORPORATION
for the
U.S. ATOMIC ENERGY COMMISSION

ANNUAL PROGRESS REPORT
TO THE
NATIONAL AERONAUTICS AND SPACE ADMINISTRATION

Title of Project:

Mutagenic Effectiveness of Known Doses of Gamma Radiation in Combination with Weightlessness on Habrobracon

For the Period:

January 1 - December 31, 1968

Principal Investigator:

R. C. von Borstel

Co-Investigators:

Roger H. Smith

Anna R. Whiting

Robert L. Amy
Department of Biology, Southwestern University, Memphis, Tennessee

Sohei Kondo
Faculty of Medicine, Osaka University, Osaka, Japan

D. S. Grosch (supported by NASA Research Grant No. NsG678)
Department of Genetics, North Carolina State University, Raleigh, North Carolina

Technical Staff:

Katherine T. Cain
Martha S. Jones
Margaret J. Lane
Joan W. Reel
Julie L. Tindall
Judith A. Winchester

Consultants:

M. B. Baird
Department of Biology, University of Delaware, Newark, Delaware

Arnold M. Clark
Department of Biology, University of Delaware, Newark, Delaware

Thomas J. Mizianty
Department of Biology, Wilkes College, Wilkes-Barre, Pennsylvania

Mary Lou Pardue
Department of Biology, Yale University, New Haven, Connecticut

Diana B. Smith
Biometrics and Statistics, Oak Ridge National Laboratory, Oak Ridge, Tennessee

L. R. Valcovic
Department of Genetics, North Carolina State University, Raleigh, North Carolina

Name of Institution:

Biology Division
Oak Ridge National Laboratory

Address:

Post Office Box Y
Oak Ridge, Tennessee 37830

Interagency Agreement:

Purchase Order ~~R-104~~ W12,792 Task No. 8

Experiment Proposal No.:

P-1079

Support:

Research jointly sponsored by the National Aeronautics and Space Administration and by the U.S. Atomic Energy Commission under contract with the Union Carbide Corporation.

PRECEDING PAGE BLANK NOT FILMED

CONTENTS

INTRODUCTION

R. C. von Borstel Roger H. Smith
Biology Division, Oak Ridge National Laboratory, Oak Ridge, Tennessee

This report summarizes the dosimetric analyses accumulated during the five-year period of the Biosatellite program. These data are from a unique source placed in a unique optical bench, the Biosatellite. Thus the multitudinous array of dosimeters was mandatory to give us confidence in the experiment.

It was especially gratifying to find that the lithium fluoride dosimetry carried out by John E. Hewitt at the Ames Research Center was in excellent agreement with our own.

ESTIMATION OF THE BACKSCATTERED FRACTION OF γ-RADIATION AND THE CONVERSION FACTORS FOR EXPOSURES OF THE HABROBRACON PACKAGES IN THE BIOSATELLITE II EXPERIMENT

Sohei Kondo[1] R. C. von Borstel Katherine T. Cain[2]

[1]Faculty of Medicine, Osaka University, Osaka, Japan, and [2]Biology Division, Oak Ridge National Laboratory, Oak Ridge, Tennessee

Extensive dosimetry testing was carried out on the space vehicle and ground-based control setup at Ames Research Center after the flight of Biosatellite II. The purpose of our experiments was to obtain data needed for converting the readings determined from Toshiba glass rods which had been loaded at different monitoring positions in the actual experiment of Biosatellite II to true exposures given to the biological materials used in our experiment. This conversion required the determination of two parameters: the fractions of exposures attributable to scattered γ-radiation, and the relative ratios of exposures at monitoring positions to those at the positions where the biological materials were loaded.

Fractions of Exposures Attributable to Scattered γ-Radiation

Principle of measurement and preparatory experiments—The reading of a glass rod exposed to primary γ-radiation contaminated with scattered γ-radiation can be expressed as

$$\underline{y} = \underline{a}\underline{P} + \underline{a}\sigma\underline{S} \qquad (1)$$

where $\underline{y}$, $\underline{P}$, and $\underline{S}$ are respectively the reading of a rod (in arbitrary units proportional to the fluorescence intensity), the exposure of primary γ-radiation, and the exposure of scattered γ-radiation; $\underline{a}$ is the rod reading per roentgen for

primary γ-radiation, and σ denotes the ratio of rod reading per roentgen of the scattered radiation to that of the primary radiation. The essential feature of the method that we used lies in the fact that the energy dependence factor, σ, and hence $\underline{y}$, takes different values for rods made of different glass or encased in different shielding material, and that the dependence of σ on energy of scattered γ-radiation is a characteristic of the glass and the shielding material.

We used high Z glass (Schulman, Ginther, Klick, Alger, and Levy, 1951) and low Z glass (Yokota, Nakajima, and Sakai, 1961). The energy dependence factor, σ, takes a maximum around 50 kev, with values of about 7 and 20 for low and high Z glasses, respectively, as shown in Figure I.1 (Fowler and Attix, 1966).

ORNL-BIO-22592

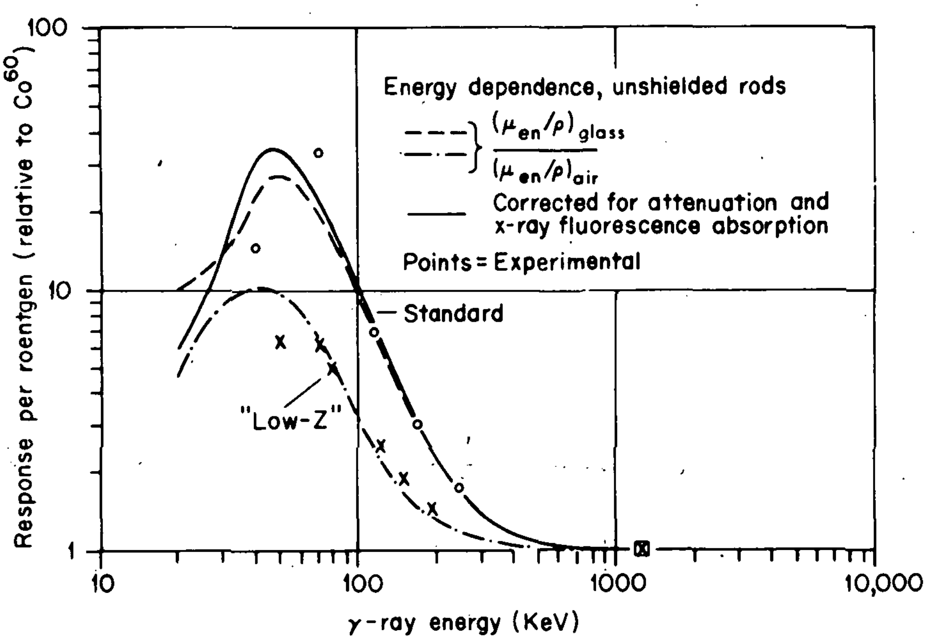

FIG. I.1. Energy-response spectrum of high Z (standard) and low Z glass rods. (After Fowler and Attix, 1966.)

This energy dependence can be greatly reduced by encasing rods in gold cases instead of plastic or other low Z material cases (Yokota and Nakajima, 1965). Combination of these factors gives four sets of dosimeters whose responses can be written as

$$\underline{y}_{\underline{i}} = \underline{a}_{\underline{i}} (\underline{P} + \sigma_{\underline{i}} \underline{S}) \qquad (\underline{i} = 1, 2, 3, 4) \qquad (2)$$

where subscripts $\underline{i}$ = 1, 2, 3, and 4 stand for the dosimeters of low Z glass rods in plastic cases, low Z in gold, high Z in plastic, and high Z in gold, respectively.

The values for $\underline{a}_{\underline{i}}$'s and $\underline{\sigma}_{\underline{i}}$'s, determined experimentally for various γ- and X-radiations with different energy spectra, are summarized in Table I.1. The low Z glass rods used in this experiment are commercially available products, 1 mm in diameter and 6 mm long, obtained from Toshiba Co. (Yokota et al., 1961). The high Z glass rods, 1 mm in diameter and 6 mm long, of the Schulman type (Schulman et al., 1951) were a gift of Dr. Ryosuke Yokota, Toshiba Co., and the gold cases were made according to the design of Yokota and Nakajima (1965) and were a gift of Toshiba Co.

Table I. 1. Relative sensitivities to various X-rays and γ-rays of glass rods encased in plastic, aluminum, and gold*

Type of Dosimeter			^{85}Sr γ-Radiation (513 kev)	180 kvp X-Radiation (1.0 mm Cu +5 mm Al filtration)	180 kvp X-Radiation (1.0 mm Al filtration)	^{241}Am X-Radiation ($\sim$60 kev)	110 kvp X-Radiation (1.0 mm Al filtration)	80 kvp X-Radiation (1.0 mm Al filtration)
$\underline{i}$†	Glass	Rod Case (wall thickness)	$\underline{a}_{\underline{i}}$‡	$\sigma_{\underline{i}}$‡	$\sigma_{\underline{i}}$	$\sigma_{\underline{i}}$	$\sigma_{\underline{i}}$	$\sigma_{\underline{i}}$
1	Low Z	Plastic (0.5 or 1.0 mm)	1.00	—	—	6.2	—	—
1'	Low Z	Aluminum (1.0 mm)	1.03	4.0	5	6.6	5.9	5.8
2	Low Z	Gold with holes (0.55 mm)	1.60	0.8	0.64	0.65	0.44	0.32
3	High Z	Plastic (0.5 or 1.0 mm)	0.858§	—	—	—	—	—
3'	High Z	Aluminum (1.0 mm)	0.88	15	17	23	19	17
4	High Z	Gold with holes (0.25 mm)	1.30	2.8	2.4	—	1.5	0.85

*These data were obtained with the help of R. Yokota and K. Hashimoto of Toshiba Company, for ^{241}Am exposure, and J. E. Hewitt, Ames Research Center, for ^{85}Sr exposure.

†This letter as a subscript specifies the type of glass and encasement as shown in columns 2 and 3.

‡$\underline{a}_{\underline{i}}$, Fluorescence intensity of dosimeter per roentgen of ^{85}Sr γ-radiation (normalized to 1.00 for $\underline{i} = 1$, i.e., made up of low Z glass encased in plastic); $\sigma_{\underline{i}}$, ratio of fluorescence intensity of a rod per roentgen of different type of X-radiation from that of ^{85}Sr γ-rays (an index of energy dependence of each glass dosimeter).

§Estimated from low Z determination.

The X-radiation used for obtaining the calibration data in Table 1 was from a tungsten target. The spectra of the X-radiation (Kondo and Kato, 1959), given in Figure I.2, were expected to simulate, though very roughly, the spectra of secondary γ-radiations (i.e., tungsten fluorescence and Compton scattering found in the Biosatellite II experiment), because the source holders for the ^{85}Sr used in the spacecraft and the ground-based control setup were made of tungsten, as were the floors of the radiation areas.

ORNL-BIO-22593

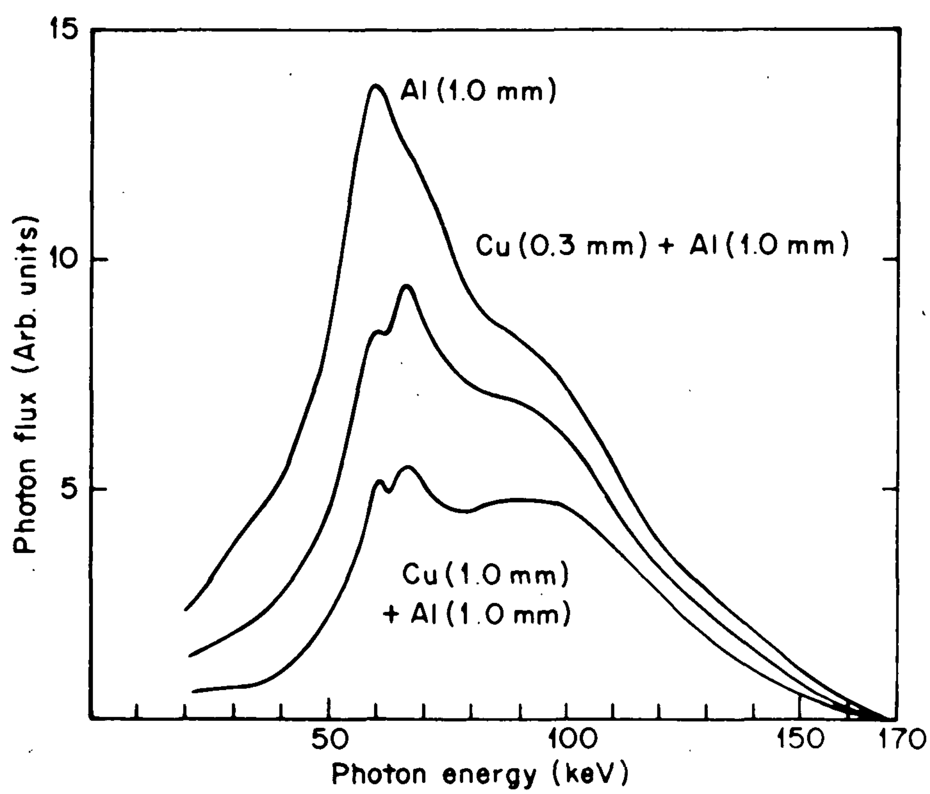

FIG. I.2. Spectrum of X-radiation believed to be similar to the scattered radiation used in present experiments (Kato and Kondo, 1959).

Experimental results with Biosatellite ground-based control and flight setups—The four packages that held the biological materials were arranged around the ^{85}Sr source (Fig. I.3) at different distances from it (Table I.2). The package in the 1-kR nominal exposure position was elevated above the tungsten backscatter shield upon an aluminum bracket; the other three packages were

ORNL-BIO-22594

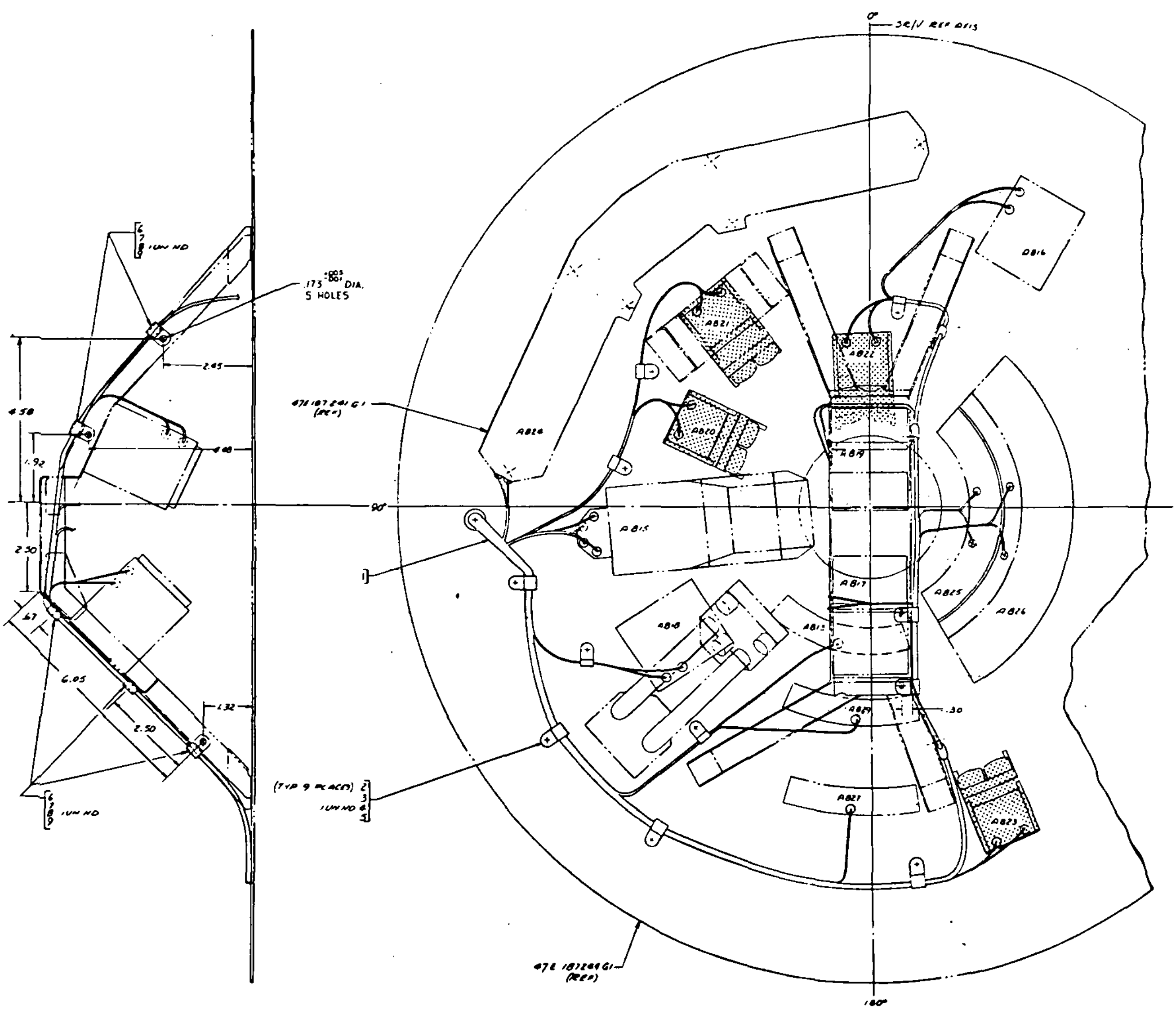

FIG. I.3. Schematic diagram of forward (radiation) section of Biosatellite II. The Habrobracon packages are shaded. The radiation source is in the geometric center.

Table I.2. Distances in centimeters of packages from the radiation source in the Biosatellite spacecraft

Package	Nominal Exposure (kR)	Maximum Distance from Source Edge to Outer Edge of Upper Right Module	Distance from Source Center to Habrobracon Position		Distance from Backscatter Shield to Package Center		Distance from Backscatter Shield to Module Center			
							Lower		Upper	
			L	1/L	H	H/L	H	H/L	H	H/L
A 822	4	6.6_1	7.9_0	0.13	3.3	0.42	2.2	0.28	4.4	0.56
A 820	2	9.7_9	11.0_7	0.09	3.3	0.30	2.2	0.20	4.4	0.40
A 821	1	13.8_8	15.1_7	0.07	6.2	0.41	5.1	0.34	7.1	0.45
A 823	0.5	21.1_9	22.4_8	0.04	3.3	0.12	2.2	0.10	4.4	0.20
Altered A 821, upper modules	1	16.2_7	17.5_6	0.06			–	–	8.6_4	0.49
Altered A 821, lower modules	1	(Lower Right Module) 11.9_1	13.1_9	0.08	7.5_2	0.49	6.4_0	0.49	–	–

H = height from backscatter shield (cm)

L = distance from source (cm)

Radius of source = 0.68_6 cm

Cap face to center of Habrobracon position = 0.6 cm

Monitor position to center of Habrobracon position = 3.5 cm

screwed to the shield. In the spacecraft, during the actual flight, the bracket of the 1-kR package was placed inadvertently in a reversed position, so that the package face was tilted at an angle 30° upward and away from the source (Figs. I.4 and I.5).

ORNL-BIO-22595

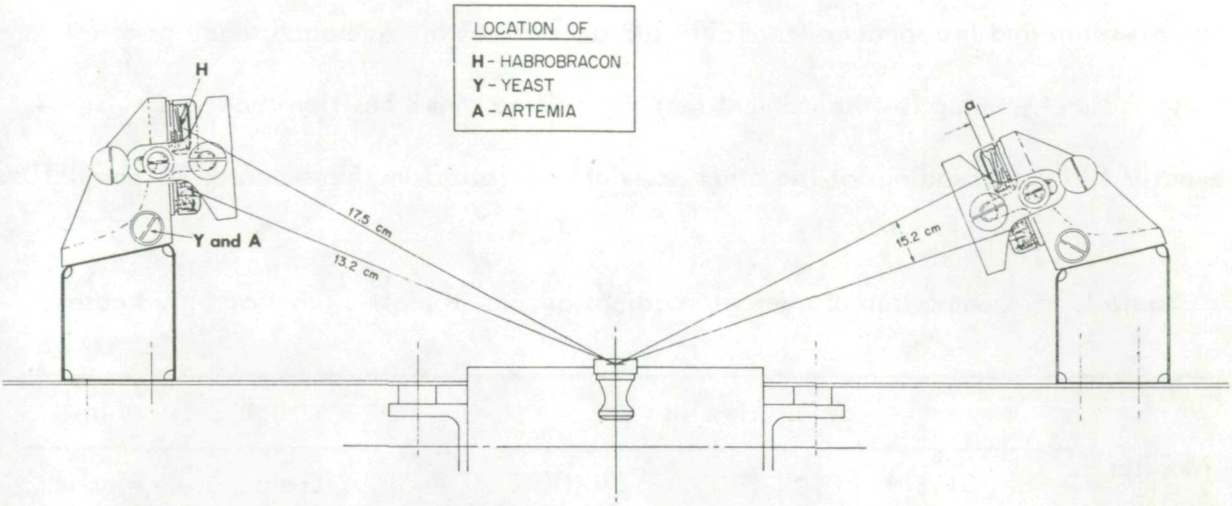

FIG. I.4. Altered and standard arrangement for Habrobracon packages at 1000-R nominal position. Distances of Habrobracon cavity, dosimeter positions, and yeast and Artemia positions, with respect to radiation source, are indicated.

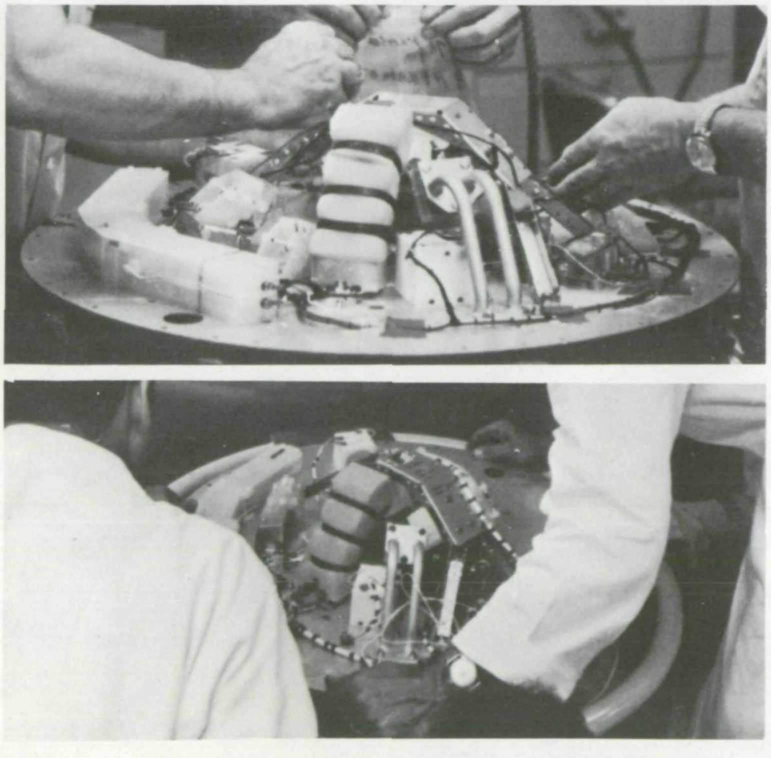

ORNL-BIO-22596

FIG. I.5. Radiation sections of ground-based control setup (above) and spacecraft (below) showing altered arrangement of Habrobracon packages at the 1-kR nominal exposure position.

We placed the four sets of glass rods at 4-kR and 0.5-kR positions in the Biosatellite ground-based control setup and in the spacecraft. Because of the shortage of the number of high Z rods at our disposal, we placed only the low Z rods encased in gold or in plastic cases at the 2-kR and 1-kR positions in the ground-based control setup and the spacecraft. Table I.3 summarizes the averaged readings of these rods. Assuming for the moment that the nominal 4-kR position received exactly 4-kR, the readings at the other positions deviate from the expected by about 10%.

Table I.3. Comparison of average readings of rods in plastic tubes and gold cases

Monitor Position	Low Z Glass in				High Z Glass in	
	Gold		Plastic		Gold	Plastic
	Measured	Ratio	Measured	Ratio	(Measured)	(Measured)
Front						
4 kR	1050 ± 26	4.0	683 ± 14	4.0	884 ± 11	627 ± 25
2 kR	502 ± 12	1.90	341 ± 4	2.0	—	—
1 kR	291 ± 9	1.12	199 ± 4	1.16	—	—
0.5 kR	148.4 ± 1.5	0.56	96.4 ± 1.7	0.56	128.4 ± 3.4	97.5 ± 4.4
Base						
0.5 kR	122 ± 4.3		80.6 ± 1.7		—	—

Substituting the reading values in Table I.3 and the values in Table I.1 for $\underline{y}$ and $\underline{a}_i$ in Equation (2), respectively, we obtain the following empirical equations:

$$\text{For the 4-kR position}\quad \begin{cases} 683 = \underline{P} + \sigma_1 \underline{S} \\ 1050 = 1.6\underline{P} + 1.6\sigma_2 \underline{S} \\ 627 = 0.858\underline{P} + 0.858\sigma_3 \underline{S} \\ 884 = 1.3\underline{P} + 1.3\sigma_4 \underline{S} \end{cases} \tag{3}$$

and

$$\text{For the 0.5-kR position}\quad \begin{cases} 96.4 = \underline{P} + \sigma_1 \underline{S} \\ 148 = 1.6\underline{P} + 1.6\sigma_2 \underline{S} \\ 97.5 = 0.858\underline{P} + 0.858\sigma_3 \underline{S} \\ 128.4 = 1.3\underline{P} + 1.3\sigma_4 \underline{S} \end{cases} \tag{4}$$

From the above equations we have

$$\underline{S} = \frac{76 \pm 32}{\sigma_3 - \sigma_2} = \frac{51 \pm 30}{\sigma_3 - \sigma_4} = \frac{48 \pm 31}{\sigma_3 - \sigma_1} \quad \text{for the 4-kR position} \tag{5}$$

$$\underline{S} = \frac{21 \pm 5}{\sigma_3 - \sigma_2} = \frac{17 \pm 5}{\sigma_3 - \sigma_1} = \frac{15 \pm 6}{\sigma_3 - \sigma_4} \quad \text{for the 0.5-kR position where the} \tag{6}$$

standard errors are calculated from the data in Table I.3. If we ignore these standard errors, from Equations (5) and (6) we have, respectively,

$$\sigma_3 > \sigma_1 > \sigma_4 > \sigma_2 \tag{7}$$

and

$$\sigma_3 > \sigma_4 > \sigma_1 > \sigma_2 \tag{8}$$

Because of the standard errors, these relations have not been strictly proved by the experimental data, but we may argue as follows: The relation $\sigma_4 > \sigma_1$, assumed at the 0.5-kR position, would be true if the component of scattered γ-rays with energy around 200 kev is much more abundant than the component with energy around 60 kev,

the energy of the tungsten fluorescence X-ray; this can be verified from the energy dependence data of σ_1 and σ_4 given in Table I.1 combined with the spectra of the X-rays used and the energy dependence spectra of σ_1 and σ_3 given in Figure I.1. The relation of $\sigma_1 > \sigma_4$ means, by similar reasoning, that the component of scattered γ-rays around 60 kev contributes more to the glass rod reading than the component around 200 kev.

From the above, or primarily theoretical argument, we may take the X-rays of 180 kvp filtered by Cu 1.0 mm + Al 0.5 mm as the first order approximation for the scattered γ-rays in the Biosatellite II, though it would have been better to have had a higher kvp X-ray machine at our disposal. Then from Table I.1 we have

$$\sigma_1 = 4.0; \sigma_2 = 0.8; \sigma_3 = 15; \sigma_4 = 2.8 \tag{9}$$

where σ_1 and σ_3 for "plastic" have been approximated by the σ_1' and σ_3' values for "aluminum" given in Table I.1. Thus substituting the values in Equation (9) for $\sigma_{\underline{i}}$'s in Equations (5) and (6), we obtain for the 4-kR position:

$$\underline{S} = 5.3 \pm 2.3; \qquad \sigma_1\underline{S} = 21 \pm 11 \tag{10}$$

and for the 0.5-kR position:

$$\underline{S} = 1.5 \pm 0.4; \qquad \sigma_1\underline{S} = 6 \pm 1.4 \tag{11}$$

where the forms of Equations (5) and (6) containing the $\sigma_3 - \sigma_2$ have been used. The other two forms gave values identical to these within the standard errors.

Since the glass rod readings were adjusted to make 1 unit of reading equal to 1 R of ^{85}Sr γ-rays, we used the following expression of factor $\underline{f}_R$ to convert the rod readings to $\underline{R}$ values:

$$\underline{f}_{\underline{R}} = \frac{\underline{P} + \underline{S}}{\underline{P} + \sigma_1 \underline{S}} = 1 - \frac{\underline{S}(\sigma_1 - 1)}{\underline{P} + \sigma_1 \underline{S}} \tag{12}$$

From Equations (3) and (5) and from (4) and (6), we have

$$\underline{f}_{\underline{R}} = 0.977 \pm 0.010, \text{ for the 4-kR position}$$

and (13)

$$\underline{f}_{\underline{R}} = 0.953 \pm 0.012, \text{ for the 0.5-kR position}$$

The $\underline{f}_{\underline{R}}$ values summarized in Table I.4 can also be used for conversion of rod readings at the "base" position, at least as the first order approximation. This is because the ratio of rod readings in gold cases to those in plastic cases at the "front" position is equal to that at the base position for the 0.5 kR position, as will be easily seen from Table I.3.

Table I.4. Estimates of the fraction of scattered radiation and the conversion factor, $\underline{f}_{\underline{R}}$, from glass rod readings to exposures for the monitoring positionings

Monitor Position	Fraction of Scattered Radiation (%)	$\underline{f}_{\underline{R}}$
4 kR	0.75	0.977
2 kR	1.1	0.97*
1 kR	1.4	0.96†
0.5 kR	1.6	0.95

*The scattered exposure fraction was interpolated from the assumed linear relationship (cf. Henry and Garrett, 1964) between the scattered exposure fraction and the H/L value where H and L are, respectively, the height of the monitor position from the floor and the distance from the source.

†Interpolated from the values at the 2-kR and 0.5-kR positions.

Scattered radiation in control (0 dose) area of spacecraft — Let us assume that no primary radiation reached the monitors in the aft area of the space vehicle behind the tungsten shield. Except for that from outside the vehicle, which was negligible, all radiation detected would then be primarily from scattering. Thus, Equation (2) for low Z rods in plastic and gold cases reduces to

$$\gamma_1 = a_1 \sigma_1 S; \quad \gamma_2 = a_2 \sigma_2 S \tag{14}$$

According to measured readings of rods in plastic and gold cases in the front position, the above equation takes the following empirical form:

$$1.3 = \sigma_1 S; \quad 0.5 = 1.6\, \sigma_2 S \tag{15}$$

Assuming that σ_2 is close to unity (Table 1), we have from Equation (15),

$$\sigma_1 \simeq 4.2; \qquad S \simeq 0.3 \text{ (R)} \tag{16}$$

This is an independent demonstration of the validity that σ_1 is close to 4, as we have assumed in the previous section.

Since the rods in the control position were exposed n times as long as those in the exposure area discussed in the previous section, the exposure to biological materials in the control can be estimated as kD_{H4}, where D_{H4} is the Habrobracon exposure for the 4-kR position and k is derived as the ratio of 0.3 R [see Equation (16)] to 667 R [see Equation (13)] divided by n.

Table 4 summarizes the values of conversion factors and fractions of exposures contributed by scattered γ-radiation relative to primary γ-radiation plus the high energy part of Compton-scattered γ-radiation. The values at 2-kR and 1-kR positions have been estimated by interpolation.

Conversion Factors for Exposures to Biological Materials

Habrobracon modules ("front" position) — The monitoring positions were 2 mm further from the source than the cavity in which the Habrobracon were placed (distance a in Fig. 4), so the conversion factor, f_H, from the reading at the monitoring position D_M to the exposure D_H given to the Habrobracon follows the equation

$$f_H = \frac{D_H}{D_M} = \left(\frac{x + a}{x}\right)^2 \simeq 1 + 2\frac{a}{x} = 1 + \frac{2ac}{\sqrt{D_H}} \qquad (17)$$

where c is a proportionality constant.

As shown in Table I.5 and plotted in Figure I.6, the experimental data nicely fit Equation (17). Table I.6 gives the best estimates of the values of f_H.

Table I.5. Rad readings at the Habrobracon position, D_H, and at the monitoring position, D_M

Nominal Position	Set	Average	Ratio (D_H/D_M)
4 kR	D_H	683 ± 14	1.09_3 (1 ± 0.023)
	D_M	625 ± 6.5	
2 kR	D_H	340.7 ± 8.9	1.05_5 (1 ± 0.012)
	D_M	323 ± 1.7	
1 kR	D_H	198.4 ± 4	1.04_9 (1 ± 0.022)
	D_M	189 ± 1.4	
0.5 kR	D_H	96.4 ± 1.7	1.02_9 (1 ± 0.019)
	D_M	93.7 ± 0.65	
Altered 1 kR	D_H	155.5 ± 3.0	1.04_4 (1 ± 0.033)
	D_M	149 ± 4.2	

Table I.6. Conversion factor, $\underline{f}_H$, from exposures at the monitoring position to those given to *Habrobracon* in the front position

Nominal Position	4 kR	2 kR	1 kR	0.5 kR	Altered 1 kR
$\underline{f}_H$	1.09	1.06	1.05	1.03	1.04

ORNL-BIO-22597

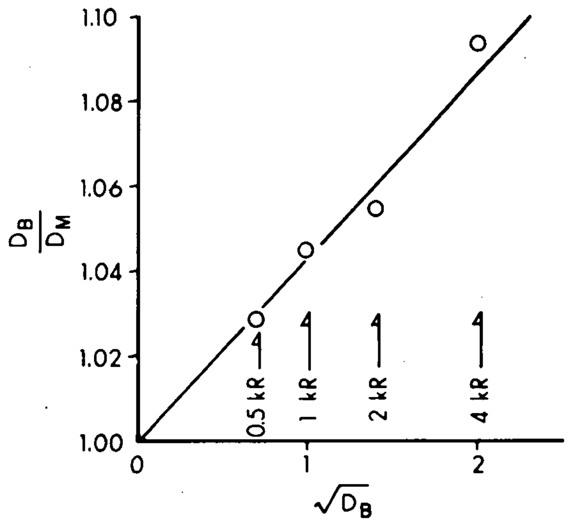

FIG. I.6. Dependence of exposure at the biological position, $\underline{D}_B$ (= $\underline{D}_H$), divided by monitoring position exposure, $\underline{D}_M$, on the square of $\underline{D}_B$.

Yeast and Artemia modules ("base" position)—The containers in which the yeast and Artemia were placed were located at the base of the packages (Fig. I.4). The exposures received in these containers were determined experimentally relative to the exposures received in the monitoring positions. The conversion factors, f_Y, are shown in Table I.7.

Table I.7. Conversion factor, f_Y, from exposures at the monitoring position to those given to yeast or Artemia at the base position

Nominal Position	"Base"	"Monitoring"	f_Y
4 kR	42.5 ± 5.6	625 ± 6.5	0.680 (1 ± 0.013)
2 kR	247 ± 2.5	323 ± 1.7	0.765 (1 ± 0.011)
1 kR	152 ± 3	189 ± 1.5	0.804 (1 ± 0.021)
0.5 kR	80.6 ± 1.7	93.7 ± 0.65	0.860 (1 ± 0.022)
Altered 1 kR	144 ± 6.5	149 ± 4.2	0.966 (1 ± 0.052)

Summary

It was shown for the Habrobracon experiment in the Biosatellite II spacecraft that the scattered radiation with an energy of less than 100 kev accounted for less than 1% of the exposure received by the 4000-R nominal exposure package. The scattered radiation accounted for less than 2% of the exposure received by the 500-R nominal exposure package.

Conversion factors were obtained which permitted us to make corrections for the geometry and the scattered radiation.

LITERATURE CITED

Fowler, J. F., and F. H. Attix, 1966, Solid state integrating dosimeters. In Radiation Dosimetry, Vol. II, Instrumentation (F. H. Attix, W. C. Roesch, and E. Tochilin, eds.), 2nd edition. Academic Press, New York, pp. 241-290.

Henry, W. H., and C. Garrett, 1964, Scattering of uncollimated cobalt-60 gamma radiation by concrete and lead barriers. Acta Radiol. Therapy Phys. Biol. 2: 353-364.

Kondo, S., and T. Kato, 1964, quoted by S. Kondo on page 683 of Chapter 15, "Radiation Dosimetry for Radiation Genetics." In Radiation Genetics (S. Matsumura and Y. Tazima, eds.). Shokabo, Tokyo, pp. 650-706.

Kondo, S., and T. Kato, 1959, Invariance of X-ray spectra at various depths in phantom. Ann. Report Natl. Inst. Genet., Japan 10: 153-154.

Schulman, J. H., R. J. Ginther, C. C. Klick, R. S. Alger, and R. A. Levy, 1951, Dosimetry of X-rays and gamma-rays by radiophotoluminescence, J. Appl. Phys. 22: 1479-1487.

Yokota, R., S. Nakajima, and E. Sakai, 1961, High sensitivity silver-activated phosphate glass for the simultaneous measurement of thermal neutrons, γ- and/or ß-rays. Health Phys. 5: 219-224.

Yokota, R., and S. Nakajima, 1965, Improved fluoroglass dosimeter as a personnel monitoring dosimeter and microdosimeter. Health Phys. 11: 241-253.

DOSIMETRIC MEASUREMENTS FOR THE BIOSATELLITE II EXPERIMENT AND ASSOCIATED AFTERFLIGHT EXPERIMENT

R. C. von Borstel Katherine T. Cain Sohei Kondo

The estimated exposures to the Habrobracon, yeast, and Artemia in the Biosatellite II experiment are summarized in Tables II.1-II.7. The exposures did not reach the nominal level because the duration of the flight was shortened. The data for each module position are the average of readings of each end of three different glass rods. The conversion from radio-photoluminescent measurements (*F*) to roetgens (*R*) is made according to

$$F = AR^{B}.$$

The constants *A* and *B* were derived experimentally from a standardized series of exposures. Below 1000 R, $A = 0.995$ and $B = 1.045$. Above 1000 R, $A = 2.146$ and $B = 0.894$. This conversion factor for exposures above 1000 R is for measurements made after 3 months when the fading of the tenebrescence of the glass has stabilized (Cheka, 1968). Below 1000 R the conversion factor changes little, if any, with time.

The corrections made in the last two columns of Tables II.5 and II.6 were necessary because the Toshiba rods used for these measurements were from a batch that was different from the batch used in the previous tests. In order to obtain proper measurements, a correction factor of 0.9445 was used.

LITERATURE CITED

Cheka, J. S., 1968, Long-term stability of radiophotoluminescence in metaphosphate glass. Health Physics **15**: 363-368.

Explanation of Tables II.1-II.7

The nominal exposure is the amount of incident radiation in roentgens that the Habrobracon were supposed to receive.

The module positions are UL (upper left), UR (upper right), LR (lower right), and LL (lower left) as seen from the ^{85}Sr source.

$\underline{T}$ is the reading of the Toshiba glass rod reader (in microamperes). The values entered in the table are twice the reading, which gives a value approximately equal to the radiation exposure in R.

f_H is the exposure in roentgens incident upon the Habrobracon.

f_Y is the exposure in roentgens incident upon the yeast and Artemia.

Table II.1. Fluorescent readings of the Toshiba glass rods in the ground-based control of the Biosatellite flight experiment of 14-17 December 1966

Nominal Exposure (R)	Module Position	2F Average Module	2F Average Horizontal (upper and lower)	2F Average Vertical (left and right)	2F Average for the Package	Average Package Exposure (R)	Corrected for Geometry and Scatter	
							f_H	f_Y
4000	UL	3809.4	3779.2	3739.8	3725.1	4200	4578	2856
	UR	3748.9		3710.3				
	LR	3671.8	3670.9					
	LL	3670.1						
2000	UL	2107.0	2113.2	2094.4	2097.5	2200	2332	1683
	UR	2119.4		2100.6				
	LR	2081.8	2081.8					
	LL	2081.8						
1000	UL	1281.7	1291.9	1271.4	1279.2	1320	1386	1061
	UR	1302.1		1286.9				
	LR	1271.7	1266.4					
	LL	1261.2						
500	UL	649.3	646.3	640.0	639.9	639.9	659	550
	UR	643.3		639.8				
	LR	636.4	633.5					
	LL	630.7						
0	UL	2.2	2.2	2.3	2.3	2.3	2.3	2.3
	UR	2.2		2.3				
	LR	2.5	2.5					
	LL	2.4						

Table II.2. Fluorescent readings of the Toshiba glass rods in the flight packages of the Biosatellite flight experiment of 7-9 September 1967

Nominal Exposure (R)	Module Position	2F Average Module	2F Average Horizontal (upper and lower)	2F Average Vertical (left and right)	2F Average for the Package	Average Package Exposure (R)	Corrected for Geometry and Scatter f_H	f_Y
4000	UL	2165.9	2187.1	2093.8	2104.6	2225	2425	1513
	UR	2208.2		2115.4				
	LR	2022.5	2022.1					
	LL	2021.6						
2000	UL	1237.3	1204.1	1191.7	1170.7	1200	1272	918
	UR	1170.8		1149.7				
	LR	1128.5	1137.3					
	LL	1146.0						
1000 Altered	UL	516.8	523.3	563.2	566.3	566.3	589	547
	UR	529.8		569.3				
	LR	608.8	609.2					
	LL	609.6						
500	UL	353.3	351.9	345.6	346.1	346.1	356	298
	UR	350.6		346.6				
	LR	342.7	340.3					
	LL	337.9						
0	UL	0.6	0.5	0.7	0.7	0.7	0.7	0.7
	UR	0.3		0.7				
	LR	1.0	0.9					
	LL	0.9						

Table II.3. Fluorescent readings of the Toshiba glass rods in the ground-based control of the Biosatellite flight experiment of 7–9 September 1967

Nominal Exposure (R)	Module Position	2F Average Module	2F Average Horizontal (upper and lower)	2F Average Vertical (left and right)	2F Average for the Package	Average Package Exposure (R)	Corrected for Geometry and Scatter $\underline{f}_H$	Corrected for Geometry and Scatter $\underline{f}_Y$
4000	UL	2151.8	2133.5	2120.7	2110.0	2230	2431	1516
	UR	2115.3		2099.3				
	LR	2083.4	2086.5					
	LL	2089.6						
2000	UL	1159.3	1147.3	1159.7	1150.8	1175	1245	899
	UR	1135.2		1141.9				
	LR	1148.5	1154.3					
	LL	1160.1						
1000	UL	719.5	709.9	693.3	694.2	694.2	729	558
	UR	700.2		695.1				
	LR	690.0	678.5					
	LL	667.1						
500	UL	365.9	367.2	357.1	360.5	360.5	371	310
	UR	368.4		363.9				
	LR	359.4	353.8					
	LL	348.2						
0	UL	1.8	1.9	1.6	1.7	1.7	1.7	1.7
	UR	2.1		1.8				
	LR	1.6	1.5					
	LL	1.4						

Table II.4. Fluorescent readings of the Toshiba glass rods in the flight packages of the phase B experiment of 12-14 March 1968

Nominal Exposure (R)	Module Position	2F Average Module	2F Average Horizontal (upper and lower)	2F Average Vertical (left and right)	2F Average for the Package	Average Package Exposure (R)	Corrected for Geometry and Scatter	
							$\underline{f}_H$	$\underline{f}_Y$
4000	UL	2092.6	2081.8	2077.3	2077.4	2180	2376	1482
	UR	2071.0		2077.5				
	LR	2084.0	2073.0					
	LL	2062.1						
2000	UL	1134.0	1140.0	1129.3	1132.0	1150	1219	880
	UR	1146.0		1134.7				
	LR	1123.4	1124.0					
	LL	1124.7						
1000	UL	668.6	672.6	656.6	656.1	656	689	527
	UR	676.6		655.5				
	LR	634.4	639.5					
	LL	644.6						
500	UL	339.3	338.1	330.0	331.8	332	342	286
	UR	337.0		333.7				
	LR	330.4	325.5					
	LL	320.7						
0	UL	1.3	1.4	1.5	1.5	1,5	1.5	1.5
	UR	1.4		1.5				
	LR	1.5	1.6					
	LL	1.7						

Table II.5. Fluorescent readings of the Toshiba glass rods in the control packages of the phase B experiment of 12–14 March 1968

Nominal Exposure (R)	Module Position	2F Average Module	2F Average Horizontal (upper and lower)	2F Average Vertical (left and right)	2F Average for the Package	Average Package Exposure (R)	Corrected for Geometry and Scatter f_H	Corrected for Geometry and Scatter f_Y
4000	UL	2144.0	2158.6	2125.8	2126.5	2240	2442	1523
	UR	2173.2		2127.2				
	LR	2081.3	2094.4					
	LL	2107.5						
2000	UL	1162.6	1167.9	1160.6	1164.1	1190	1261	910
	UR	1173.2		1167.5				
	LR	1161.9	1160.2					
	LL	1158.6						
1000	UL	707.7	696.5	699.6	688.6	689	723	554
	UR	685.3		677.6				
	LR	670.0	680.7					
	LL	691.5						
500	UL	337.0	338.1	330.9	331.2	331	341	285
	UR	339.3		331.5				
	LR	323.7	324.3					
	LL	324.9						
0	UL	1.5	1.6	1.6	1.5	1.5	1.5	1.5
	UR	1.7		1.5				
	LR	1.3	1.5					
	LL	1.7						

Table II.6 Fluorescent readings of the Toshiba glass rods in the flight packages of the phase C experiment of 22-24 May 1968

Nominal Exposure (R)	Module Position	2F Average Module	2F Average Horizontal (upper and lower)	2F Average Vertical (left and right)	2F Average for the Package	Average Package Exposure (R)	Corrected for Geometry and Scatter $\underline{f}_H$	Corrected for Geometry and Scatter $\underline{f}_Y$	Corrected for Rod Sensitivity* $\underline{f}_H$	Corrected for Rod Sensitivity* $\underline{f}_Y$
4000	UL	2264.4	2280.2	2221.5	2247.2	2400	2616	1632	2471	1541
	UR	2295.9		2272.9						
	LR	2249.8	2214.2							
	LL	2178.5								
2000	UL	1201.0	1212.1	1196.0	1203.3	1230	1304	941	1232	889
	UR	1223.2		1210.6						
	LR	1198.0	1194.5							
	LL	1191.1								
1000	UL	553.6	555.5	583.7	585.6	586	609	566	575	535
	UR	557.5		587.6						
	LR	617.7	615.7							
	LL	613.8								
500	UL	365.6	366.4	361.2	361.9	362	373	311	352	294
	UR	367.3		362.6						
	LR	358.0	357.4							
	LL	356.7								
0	UL	1.7	1.8	1.7	1.8	1.8	1.8	1.8	1.7	1.7
	UR	1.9		1.9						
	LR	1.8	1.8							
	LL	1.7								

*Correction factor for rod sensitivity = 0.9445

Table II.7. Fluorescent readings of the Toshiba glass rods in the control packages of the phase C experiment of 22-24 May 1968

Nominal Exposure (R)	Module Position	2F Average Module	2F Average Horizontal (upper and lower)	2F Average Vertical (left and right)	2F Average for the Package	Average Package Exposure (R)	Corrected for Geometry and Scatter $\underline{f}_H$	Corrected for Geometry and Scatter $\underline{f}_Y$	Corrected for Rod Sensitivity* $\underline{f}_H$	Corrected for Rod Sensitivity* $\underline{f}_Y$
4000	UL	2161.9	2199.9	2187.9	2216.6	2350	2562	1598	2420	1509
	UR	2237.9		2245.3						
	LR	2252.8	2233.4							
	LL	2214.0								
2000	UL	1205.3	1211.9	1211.5	1205.9	1240	1314	949	1241	896
	UR	1218.6		1200.3						
	LR	1182.1	1199.9							
	LL	1217.6								
1000	UL	737.5	740.6	732.2	732.6	733	769	589	726	556
	UR	743.7		733.0						
	LR	722.3	724.6							
	LL	726.8								
500	UL	373.5	377.8	365.9	370.4	370	381	318	360	300
	UR	382.1		374.9						
	LR	367.7	363.0							
	LL	358.4								
0	UL	1.4	1.5	1.5	1.5	1.5	1.5	1.5	1.4	1.4
	UR	1.6		1.5						
	LR	1.5	1.5							
	LL	1.6								

*Correction factor for rod sensitivity = 0.9445

INTRA-EXPERIMENTAL DOSIMETRIC COMPARISONS

R. C. von Borstel Diana B. Smith[1] John E. Hewitt[2]

[1]Biometrics and Statistics, Oak Ridge National Laboratory, Oak Ridge, Tennessee, and
[2]Biosatellite Project, Ames Research Center, Moffet Field, California

The comparisons of the dosimetric data taken from the Toshiba glass rods and lithium fluoride are shown in Figure III. 1. They are based on data obtained from the Biosatellite flight itself. If the data from the altered package (1000-R nominal exposure during the flight) are discounted, the data for the glass rods and the Lif powder from the Biosatellite spacecraft and earth-based control follow inverse-square relations reasonably well. For the slightly higher reading shown by the Lif in the tube closest to the radiation source, we believe that the Lif received a slightly higher exposure, since it was in a tube that formed a chord transecting the isodose line. The glass rods in the package nearest the source were on a surface that was the arc of the isodose line itself. Further away from the source, the dosimeters, even including the tubes, were within 5% of the isodose lines.

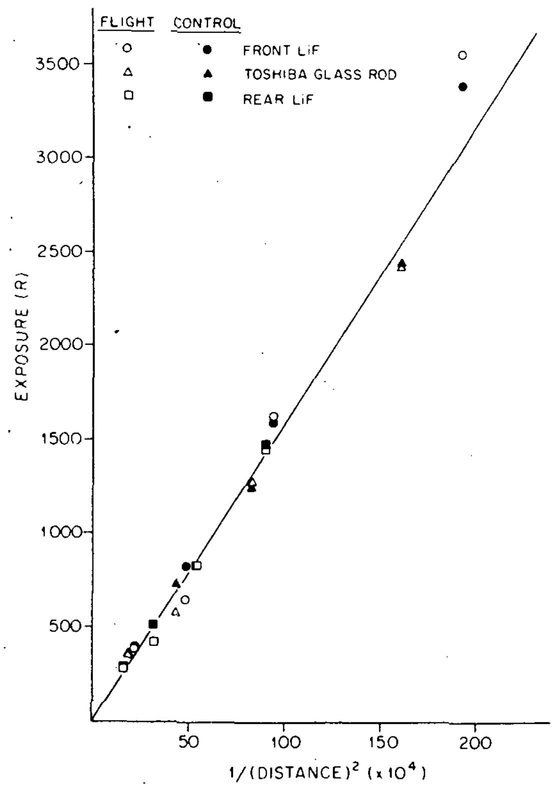

ORNL-BIO-23106

FIG. III. 1. Exposure-distance relations for the Habrobracon packages in the Biosatellite II experiment.

INTERNAL DISTRIBUTION

1.	H. I. Adler	42-151.	Roger H. Smith
2.	S. F. Carson	152.	Anna R. Whiting
3-22.	F. J. de Serres	153.	A. M. Weinberg
23.	W. H. Jordan	154-164.	Biology Division Editorial Office
24.	R. F. Hibbs	165.	Biology Library
25-34.	J. L. Liverman	166-167.	Central Research Library
35.	A. J. Miller	168.	ORNL – Y-12 Technical Library Document Reference Section
36.	J. A. Auxier	169-173.	Laboratory Records Department
37.	R. A. McNees	174.	Laboratory Records ORNL RC
38.	H. G. MacPherson	175.	ORNL Patent Office
39-40.	R. B. Parker		
41.	Diana B. Smith		

EXTERNAL DISTRIBUTION

176. Dr. R. L. Amy, Department of Biology, Southwestern University, Memphis, Tennessee 38112
177-182. Dr. N. Barr, Division of Research, U.S. Atomic Energy Commission, Washington, D.C. 20545
183. Dr. A. M. Clark, Department of Biology, University of Delaware, Newark, Delaware 19711
184. Dr. John R. Totter, Director, Division of Biology and Medicine, U.S. Atomic Energy Commission, Washington, D.C. 20545
185. Dr. C. W. Edington, Chief, Biology Branch, Division of Biology and Medicine, U.S. Atomic Energy Commission, Washington, D.C. 20545
186. Dr. R. F. Kimball, U.S. Atomic Energy Commission, Washington, D.C. 20545
187. Dr. D. S. Grosch, Department of Genetics, North Carolina State University, Raleigh, North Carolina 27607
188. Dr. John E. Hewitt, Ames Research Center, Moffett Field, California 94035
189. Capt. Walter Jones, Director, Biotechnology and Human Research, Office of Advanced Research and Technology, NASA, Washington, D.C. 20546
190. Dr. W. Keller, Space Vehicle Research and Technology, Office of Advanced Research and Technology, NASA, Washington, D.C. 20546

191. Dr. Sohei Kondo, Faculty of Medicine, Osaka University, Osaka, Japan
192. Dr. L. E. LaChance, Metabolism and Radiation Research Laboratory, USDA, State University Station, Fargo, North Dakota 58102
193-217. Miss Winnie M. Morgan, Technical Reports Office, Grants and Research Contracts, Office of Space Sciences, NASA, Washington, D.C. 20546
218-242. Mr. T. Smull, Director, Grants and Research Contracts, Office of Space Sciences, NASA, Washington, D.C. 20546
243. Dr. John W. Tremor, Ames Research Center, Moffett Field, California 94035
244. Mr. L. R. Valcovic, Department of Genetics, North Carolina State University, Raleigh, North Carolina 27607
245-246. Biotechnology and Human Research, Office of Advanced Research and Technology, NASA, Washington, D.C. 20546
247-249. Director, Bio-Science Programs, Office of Space Sciences, NASA, Washington, D.C. 20546
250-251. Technical Information Center, Oak Ridge, Tennessee 37830
252. Laboratory and University Division, AEC, ORO, Oak Ridge, Tennessee 37830
253. Dr. Thomas J. Mizianty, Department of Biology, Wilkes College, Wilkes-Barre, Pennsylvania 18703